Supplementary Material Cover Sheet

Insight into the effect of citric acid on carbon dots-mediated transport of Cd^{2+} through saturated porous media

Haojing Zhang [1, 2, a], Taotao Lu [3, a], Jiuyan Chen [2], Qiang Zhang [2], Yanxiang Li [4],
Weifeng Chen [1,*], and Zhichong Qi [2,**]

[1] Key Laboratory for Humid Subtropical Eco-geographical Processes of the Ministry of Education/ Fujian Provincial Key Laboratory for Plant Eco-physiology/ School of Geographical Sciences, Fujian Normal University, Fuzhou, Fujian 350007, China

[2] Henan Joint International Research Laboratory of Environmental Pollution Control Materials, College of Chemistry and Chemical Engineering, Henan University, Kaifeng 475004, China

[3] College of Water Resources & Civil Engineering, Hunan Agricultural University, Changsha, 410128, China

[4] The Testing Center of Shandong Bureau of China Metallurgical Geology Bureau, Jinan 250014, China

Manuscript prepared for *Environmental Science: Nano*

[*] Corresponding author: Weifeng Chen (fengweichen1986@163.com);

[**] Corresponding author: Zhichong Qi (qizhichong1984@163.com).

[a] Haojing Zhang and Taotao Lu contributed equally.

Number of pages: 26

Number of tables: 10

Number of figures: 7

S1. Deposition rate coefficient (*k*$_d$) and attachment efficiency (*α*).

The deposition rate coefficient (k_d, min^{-1}) is determined by the equation:[S1, S2]

$$k_d = -\frac{U}{\varepsilon L}\ln\left(\frac{C}{C_0}\right) \tag{S1}$$

where U is pore water velocity (cm/min), L is the filter medium packed length (cm), ε is the porosity of the sand, C/C_0 is the column outlet normalized particle concentration at the initial stage of the particle breakthrough curve.[S3, S4]

The obtained k_d was then used to calculate the attachment efficiency (α):[S5, S6]

$$\alpha = \frac{2k_d \varepsilon d_c}{3(1-\varepsilon)U\eta_0} \tag{S2}$$

where d_c is mean grains radius (cm) and η_0 is the predicted single-collector contact efficiency. η_0 can be calculated by the correlation developed by Tufenkji and Elimelech.[S1]

S2. Adsorption studies of Cd^{2+} onto sand

A batch sorption method was adopted to investigate the effects of citric acid/CDs on the binding affinities of Cd^{2+} to quartz sand.

In the absence of CDs, briefly, approximately 5 g of quartz sand and 20 mL of Cd^{2+} solution (1 mg/L) with or without LMWOAs (0.5 mM NaCl) were placed into 20-ml amber glass vials. The experimental solution pH values were adjusted by 0.1 M NaOH or HCl solutions. These vials were equilibrated for 10 h by horizontally shaking (the duration equals column experiment). The vials were then centrifuged at 5000 rpm for 20 min and the supernatants were withdrawn to obtain the concentrations of Cd^{2+} in the aqueous solution, using an ICP-OES instrument. All experiments were run in triplicate. The distribution coefficients of Cd^{2+}, K_d (L/kg), between sand and water were calculated by using the equation: $K_d = q/C_e$, where q (mg/kg) was the concentration of Cd^{2+} adsorbed on the sand. In addition, C_e (mg/L) was the concentration of Cd^{2+} in the solution.

In the presence of CDs, first, a series of dialysis bags (500 Da), each containing approximately 3 ml of 0.5 mM aqueous NaCl solution, were stored in 100 mL amber glass screw-capped vials containing different concentrations of CDs (5–30 mg L^{-1}), 1 mg L^{-1} Cd^{2+} solution, citric acid of various concentrations, and 25 g of quartz sand. The experimental solution pH values were adjusted by 0.1 M NaOH or HCl solutions. Afterward, the amber glass vials were stocked on an orbital shaker and tumbled for 10 h (the duration equals column experiment). Then, the concentrations of Cd^{2+} inside of the dialysis bags were determined by ICP-OES. Note that these concentrations were the freely dissolved concentrations of the metal ions (C_e). The concentrations of Cd^{2+} adsorbed to sand were calculated based on a mass balance approach (i.e., $m_{\text{adsorbed } Cd^{2+}} = m_{\text{initial } Cd^{2+}} - m_{\text{adsorbed } Cd^{2+} \text{onto CDs}} - m_{\text{free } Cd^{2+}}$, note that $m_{\text{adsorbed } Cd^{2+} \text{onto CDs}}$ was obtained based on the sorption experiments described in Section 2.4). All experiments were run in triplicate. The distribution coefficients of Cd^{2+} (K_d (L/kg)) were calculated by using the equation as mentioned above.

S3. Adsorption studies of citric acid onto sand

Adsorption studies were conducted to determine the adsorption capacity of citric acid onto sand under different pH conditions. Frist, approximately 5 g quartz sand and 20 mL of organic acid solutions (0.1 mM) were added to each of a series of 20-ml amber glass vials. Then, the vials were equilibrated for 10 h by horizontally shaking (the duration equal to the transport experiment). Then, the vials were centrifuged at 5000 rpm for 20 min, and the supernatants were withdrawn. The concentration of citric acid was analyzed by a total organic carbon analyzer from Shimadzu Scientific (Columbia, MD, USA). The adsorbed citric acid on sand grains (q (μmol/kg)) was then determined by the difference between the initial and final citric acid concentrations in the aqueous phase. All experiments were run in triplicate.

S4. Adsorption of citric acid onto CDs

Adsorption experiments were conducted to determine the adsorption capacity of citric acid onto CDs under different conditions. First, a series of dialysis bags (500 Da), each containing approximately 3 ml of 0.5 mM aqueous NaCl solution, were stored in 100 mL amber glass screw-capped vials containing different concentrations of CDs (5–30 mg L^{-1}), citric acid of various concentrations, and 25 g of quartz sand. The experimental solution pH values were adjusted by 0.1 M NaOH or HCl solutions. Afterward, the amber glass vials were stocked on an orbital shaker and tumbled for 10 h (the duration equals column experiment). Then, the concentration of citric acid inside of the dialysis bags was analyzed by a total organic carbon analyzer from Shimadzu Scientific (Columbia, MD, USA). The concentrations of citric acid adsorbed to CDs (q (μmol/g)) were calculated based on a mass balance approach (i.e., $m_{\text{adsorbed citric acid}} = m_{\text{initial citric acid}} - m_{\text{adsorbed citric acid onto sand}} - m_{\text{free citric acid}}$; note that $m_{\text{adsorbed citric acid onto sand}}$ was obtained based on the sorption experiments described in Section S3). All experiments were run in triplicate.

S5. Transport model

The simulation model had been commonly used to predict the transport behavior of Cd^{2+}. The program CXTFIT 2.0 was used to fit the Cd^{2+} experimental breakthrough curves.[S7] In this model, two different types of sorption were assumed: kinetic and the equilibrium.[S8] The model can be explained in Eqs. S3–S6.

$$\beta R\frac{\partial C_1}{\partial T}=\frac{1}{P}\frac{\partial^2 C_1}{\partial X^2}-\frac{\partial C_1}{\partial X}-\omega(C_1-C_2) \tag{S3}$$

$$(1-\beta)R\frac{\partial C_2}{\partial T}=\omega(C_1-C_2) \tag{S4}$$

where parameters without dimensions are as follows:

$$X=\frac{x}{L} \tag{S5}$$

$$P=\frac{vL}{D} \tag{S6}$$

where C_1 and C_2 (mg/L) are the solute concentrations in sorption sites 1 and 2 respectively, T (d) is the time and L (m) is the column length; X is the vertical spatial coordinate; D (m^2/d) is the hydrodynamic dispersion coefficient; P is the Peclet number. R is the retardation factor; β represents the fraction of the instantaneous equilibrium adsorption sites in all the adsorption sites;[S9] and ω is the Damkohler number, indicating the ratio of the reaction rate to the transport rate.[S10] By fitting conservative tracer (KBr) curves using the 2.1 code of CXTFIT, the value for dispersion coefficient (D) was evaluated (Fig. S2).[S7] We supposed that the D value of Cd^{2+} is the same as that in the sand column for the bromide.[S11] By matching the breakthrough curve of the Cd^{2+}, the value of R, β and ω was achieved.

Table S1. Structures and acidity coefficient (pK_a) of citric acid.

Organic acid	Structure	Molecular weight	pK_{a1}	pK_{a2}	pK_{a3}

Citric acid	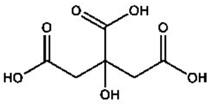	192.14	3.13	4.76	6.40

Table S2. Experimental protocols of column tests

Column No.	CDs conc. [a] (mg/L)	Cd^{2+} conc. [a] (mg/L)	background solution	pH	porosity (-)	bulk density (g/cm^3)
1	0	1	0.5 mM NaCl	7.0	0.48	1.38
2	5	1	0.5 mM NaCl	7.0	0.48	1.38
3	10	1	0.5 mM NaCl	7.0	0.48	1.37
4	30	1	0.5 mM NaCl	7.0	0.48	1.37
5	5	1	0.5 mM NaCl + 0.1 mM citric acid	7.0	0.48	1.37
6	5	1	0.5 mM NaCl + 0.3 mM citric acid	7.0	0.48	1.37
7	5	1	0.5 mM NaCl + 0.5 mM citric acid	7.0	0.48	1.37
8	5	1	0.5 mM NaCl + 0.1 mM citric acid	6.0	0.49	1.36
9	5	1	0.5 mM NaCl + 0.1 mM citric acid	8.0	0.48	1.38

[a] conc. represent concentration.

Table S3. X-ray photoelectron spectroscopy (XPS) analysis of CDs.

	Peak Binding Energy	wt. (%)
C-C/C=C	284.43	43.26
Oxygenated carbon	285.63	29.36
Nitrous carbon	287.27	27.38

Table S4. Adsorption amount of Cd^{2+} onto CDs under different solution chemsitry conditions. Error bars represent standard deviations from replicate experiments (n=3)

No.	background solution	CDs conc. [a] (mg/L)	pH	*q* (mg/g)
1	0.5 mM NaCl	5	7.0	34.7 ± 0.5
2	0.5 mM NaCl	10	7.0	26.1 ± 3.2
3	0.5 mM NaCl	30	7.0	21.6 ± 1.3
4	0.5 mM NaCl + 0.1 mM citric acid	5	7.0	44.9 ± 0.4
5	0.5 mM NaCl + 0.3 mM citric acid	5	7.0	65.1 ± 1.2
6	0.5 mM NaCl + 0.5 mM citric acid	5	7.0	77.0 ± 11.6
7	0.5 mM NaCl + 0.1 mM citric acid	5	6.0	28.4 ± 5.3
8	0.5 mM NaCl + 0.1 mM citric acid	5	8.0	83.9 ± 2.6

[a] conc. represent concentration.

Table S5. ζ-potential of CDs under different solution chemistry conditions

No.	Background solution	pH	ζ-potential of CDs (mV) [a]	ζ-potential of sand (mV)
1	0.5 mM NaCl	7.0	-2.14 ± 0.4	-52.9 ± 0.4
2	0.5 mM NaCl + 0.1 mM citric acid	7.0	-2.59 ± 1.2	-53.3± 0.9
3	0.5 mM NaCl + 0.3 mM citric acid	7.0	-4.28 ±2.1	-57.8 ±2.3
4	0.5 mM NaCl + 0.5 mM citric acid	7.0	-15.9 ± 0.2	-59.0 ±1.4
5	0.5 mM NaCl + 0.1 mM citric acid	6.0	-1.32 ± 0.1	-49.2 ± 0.4
6	0.5 mM NaCl + 0.1 mM citric acid	8.0	-9.83± 2.2	-55.0 ± 2.7

[a] the concentration of CDs was 5 mg/L.

Table S6. Attachment efficiencies (α) and deposition rate coefficients (k_d) of the column transport experiments

column No.	CDs conc. (mg L^{-1}) [a]	Cd^{2+} conc. (mg L^{-1}) [a]	background solution	pH	attachment efficiencies (α)	deposition rate coefficients (k_d, min^{-1})
1	0	1	0.5 mM NaCl	7.0	/	/
2	5	1	0.5 mM NaCl	7.0	1.04E-01	1.81E-03
3	10	1	0.5 mM NaCl	7.0	5.66E-02	7.74E-04
4	30	1	0.5 mM NaCl	7.0	1.41E-02	1.83E-04
5	5	1	0.5 mM NaCl + 0.1 mM citric acid	7.0	4.92E-02	7.28E-04
6	5	1	0.5 mM NaCl + 0.3 mM citric acid	7.0	2.86E-02	4.35E-04
7	5	1	0.5 mM NaCl + 0.5 mM citric acid	7.0	1.80E-02	3.03E-04
8	5	1	0.5 mM NaCl + 0.1 mM citric acid	6.0	6.47E-02	9.12E-04
9	5	1	0.5 mM NaCl + 0.1 mM citric acid	8.0	1.96E-02	3.03E-04

[a] conc. represent concentration.

Table S7. The adsorption coefficients (K_d) of Cd^{2+} (1 mg/L) to sand.

column No.	CDs conc. (mg L^{-1}) [a]	Cd^{2+} conc. (mg L^{-1}) [a]	background solution	pH	K_d (L/kg)
1	0	1	0.5 mM NaCl	7.0	3.56 ± 0.15
2	5	1	0.5 mM NaCl	7.0	2.28 ± 0.18
3	10	1	0.5 mM NaCl	7.0	2.03 ± 0.07
4	30	1	0.5 mM NaCl	7.0	1.96 ± 0.11
5	5	1	0.5 mM NaCl + 0.1 mM citric acid	7.0	1.82 ± 0.13
6	5	1	0.5 mM NaCl + 0.3 mM citric acid	7.0	1.75 ± 0.09
7	5	1	0.5 mM NaCl + 0.5 mM citric acid	7.0	1.70 ± 0.12
8	5	1	0.5 mM NaCl + 0.1 mM citric acid	6.0	1.63 ± 0.21
9	5	1	0.5 mM NaCl + 0.1 mM citric acid	8.0	1.98 ± 0.05

Table S8. Fitted parameters of two-site nonequilibrium transport model from breakthrough results of column experiments.

column No.	CDs conc. (mg L^{-1}) [a]	Cd^{2+} conc. (mg L^{-1}) [a]	background solution	pH	Parameters of two-site nonequilibrium transport model			
					R (-)	*β* (-)	*ω* (-)	r^2
1	0	1	0.5 mM NaCl	7.0	4.93 ± 0.25	0.617 ± 0.029	0.406 ± 0.089	0.995
2	5	1	0.5 mM NaCl	7.0	2.89 ± 0.12	0.815 ± 0.105	0.185 ± 0.027	0.991
3	10	1	0.5 mM NaCl	7.0	1.99 ± 0.15	0.865 ± 0.078	0.122 ± 0.023	0.987
4	30	1	0.5 mM NaCl	7.0	1.52 ± 0.29	0.886 ± 0.102	0.085 ± 0.015	0.989
5	5	1	0.5 mM NaCl + 0.1 mM citric acid	7.0	2.65 ± 0.23	0.823 ± 0.122	0.173 ± 0.036	0.991
6	5	1	0.5 mM NaCl + 0.3 mM citric acid	7.0	2.12 ± 0.09	0.871 ± 0.013	0.115 ± 0.027	0.992
7	5	1	0.5 mM NaCl + 0.5 mM citric acid	7.0	1.77 ± 0.27	0.899 ± 0.056	0.082 ± 0.012	0.993
8	5	1	0.5 mM NaCl + 0.1 mM citric acid	6.0	1.86 ± 0.23	0.875 ± 0113	0.155 ± 0.031	0.989
9	5	1	0.5 mM NaCl + 0.1 mM citric acid	8.0	3.25 ± 0.35	0.769 ± 0.105	0.189 ± 0.059	0.995

[a] conc. represent concentration.

Table S9. Adsorption amount of citric acid onto sand under different pH conditions. Error bars represent standard deviations from replicate experiments (n=3)

citric acid conc.	Electrolyte solution	pH	*q* (mmol-citric acid/kg-sand)
0.1 mM	0.5 mM NaCl	7.0	0.11 ± 0.01
0.3 mM	0.5 mM NaCl	7.0	0.13 ± 0.05
0.5 mM	0.5 mM NaCl	7.0	0.16 ± 0.03
0.1 mM	0.5 mM NaCl	6.0	0.13 ± 0.02
0.1 mM	0.5 mM NaCl	8.0	0.09 ± 0.03

Table S10. Adsorption amount of citric acid onto CDs under different pH conditions. Error bars represent standard deviations from replicate experiments (n=3)

citric acid conc.	Electrolyte solution	pH	*q* (μmol-citric acid/g-CDs)
0.1 mM	0.5 mM NaCl	7.0	8.5 ± 0.2
0.3 mM	0.5 mM NaCl	7.0	12.5 ± 1.1
0.5 mM	0.5 mM NaCl	7.0	22.1 ± 0.9
0.1 mM	0.5 mM NaCl	6.0	9.9 ± 0.5
0.1 mM	0.5 mM NaCl	8.0	6.3 ± 0.3

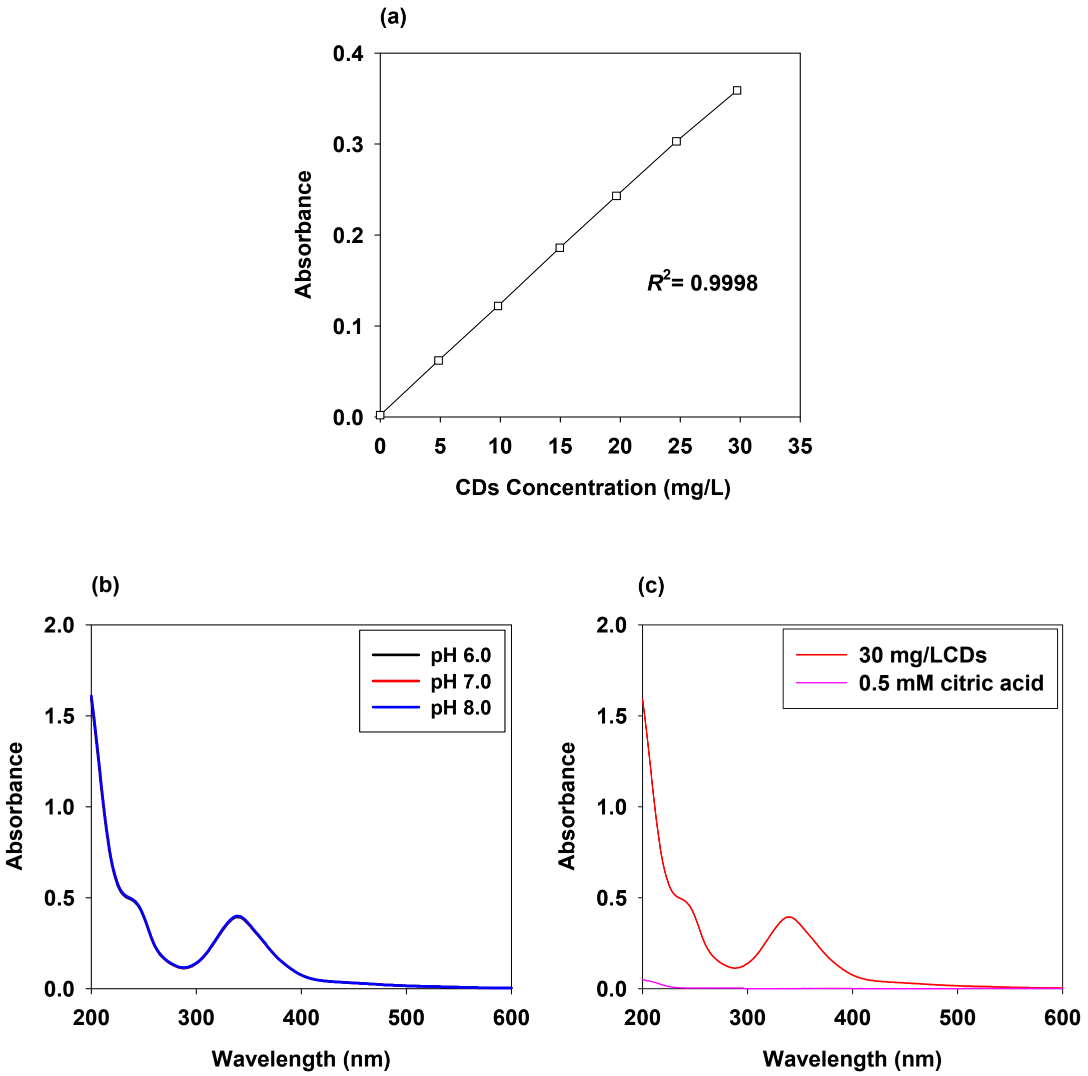

Fig. S1. (a) Calibration curve as absorbance vs. concentrations of CDs in suspension (absorbance at the wavelength of 335 nm); (b) Effects of solution pH on UV absorbance of CDs; (c) UV/Vis spectra of CDs (30 mg/L) and citric acid (0.5 mM) dispersed in DI water.

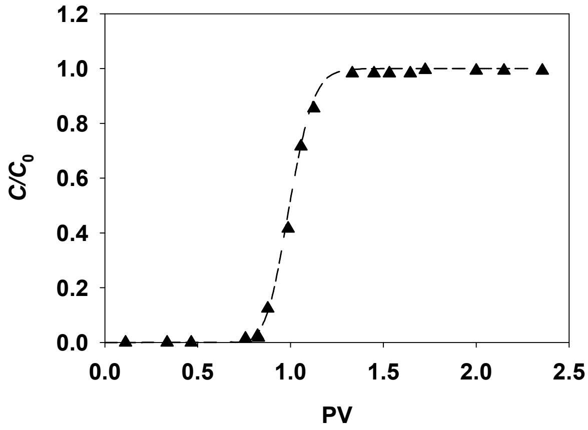

Fig. S2. The representative breakthrough curve of conservative tracer (Br^-). The line was plotted by fitting the breakthrough data with the one-dimensional steady-state advection-dispersion equation**.**

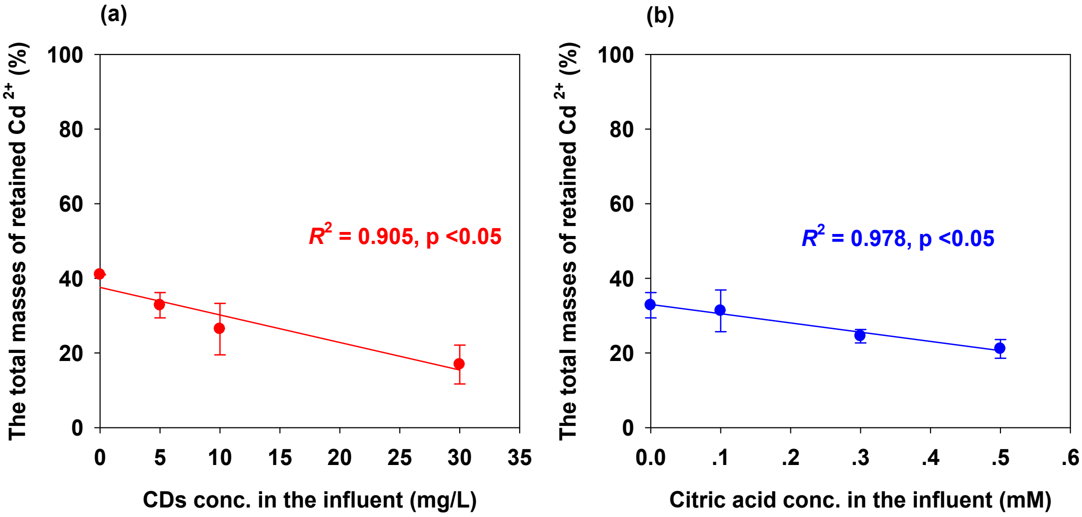

Fig. S3. (a) Comparison between the total masses of retained Cd^{2+} in the columns and concentration of CDs in the influent (without citric acid) for columns 1–4; (b) Comparison between the total masses of retained Cd^{2+} in the columns and concentration of citric acid in the influent (in the presence of 5 mg/L CDs) for columns 2, and 5–7.

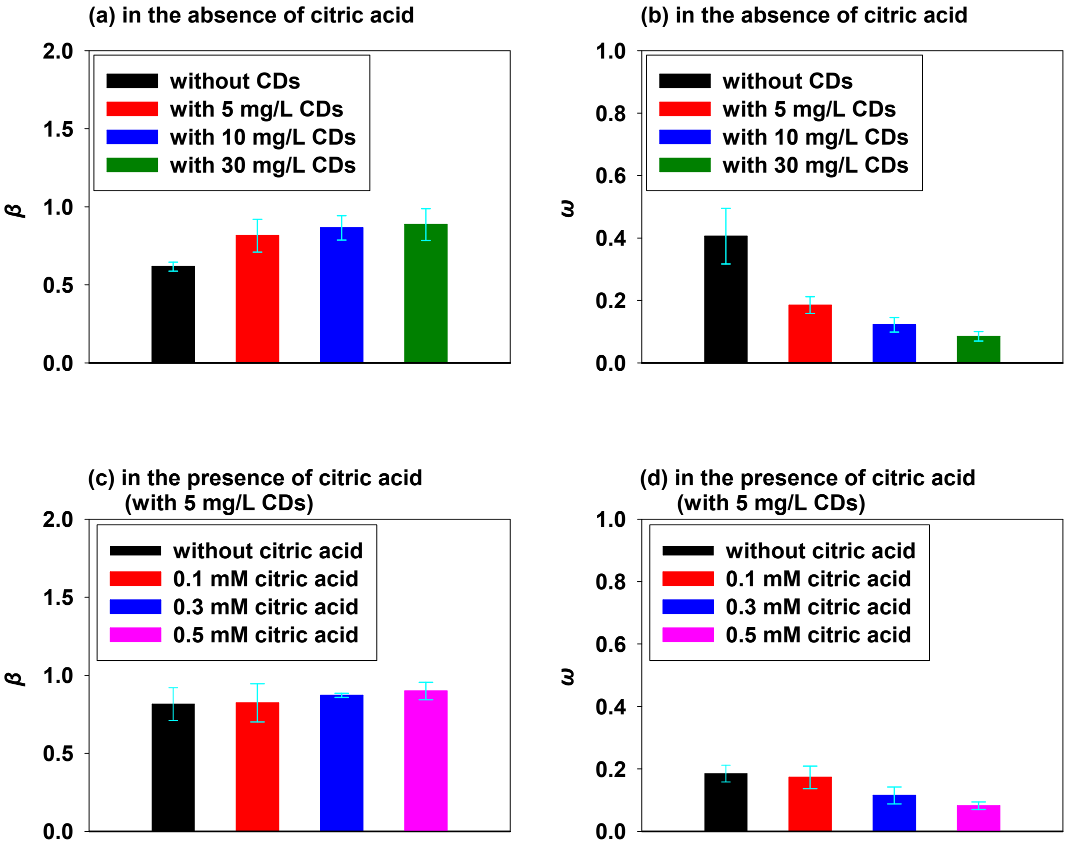

Fig. S4. Fitted parameters of two-site nonequilibrium transport model from breakthrough results of column experiments: (a) the fraction of instantaneous retardation to the total retardation in the absence of citric acid; (b) the coefficient of partitioning between the equilibrium and nonequilibrium phases in the absence of citric acid; (c) the fraction of instantaneous retardation to the total retardation in the presence of citric acid with 5 mg/L CDs; and (d) the coefficient of partitioning between the equilibrium and nonequilibrium phases in the presence of citric acid with 5 mg/L CDs.

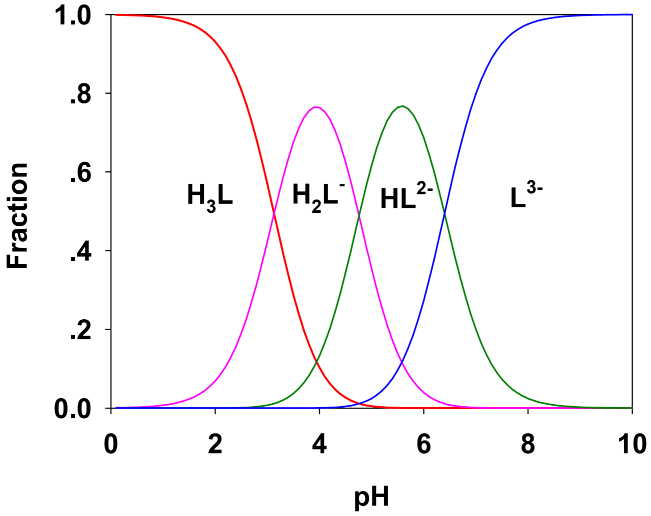

Fig. S5. pH-dependent speciation of the whole citric acid (denoted as H_3L, L represents ligand) molecular and the functional groups, respectively.

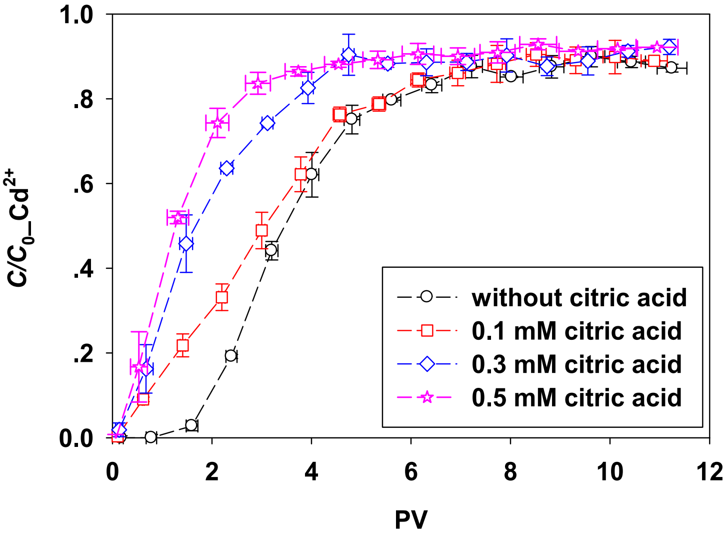

Fig. S6. Effects of citric acid on the transport of Cd^{2+} (1 mg/L) at pH 7.0.

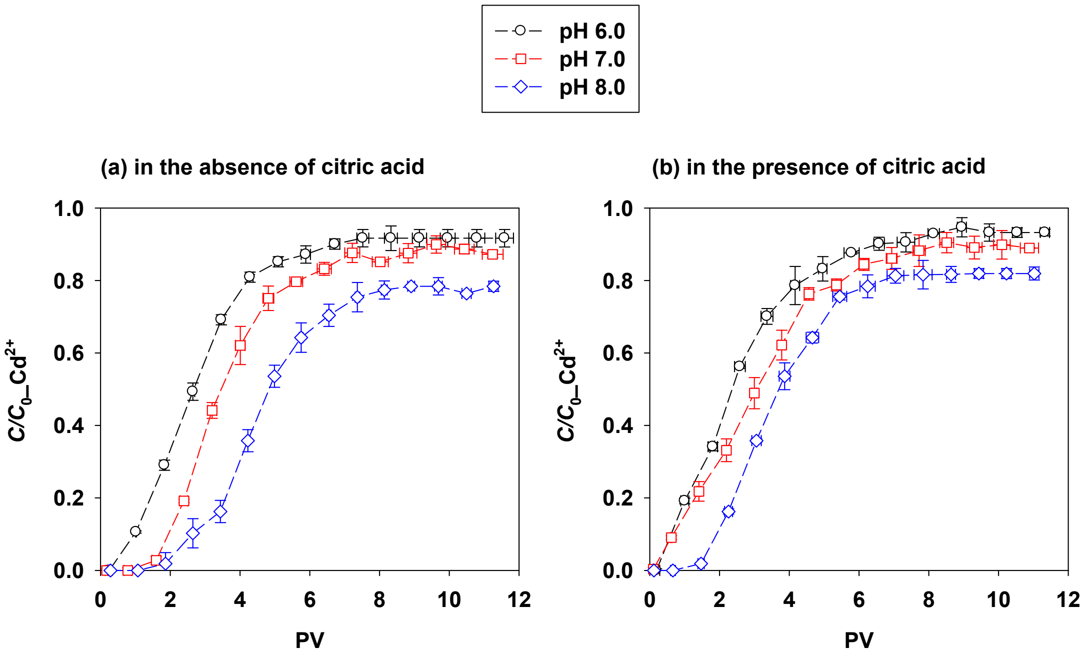

Fig. S7. Transport of Cd^{2+} (1 mg/L) with or without citric acid (0.1 mM) at different solution pH conditions.

References:

S1. N. Tufenkji and M. Elimelech, Correlation equation for predicting single-collector efficiency in physicochemical filtration in saturated porous media, *Environ. Sci. Technol.*, 2004, **38,** 529−536.

S2. J. Zhuang, J. Qi and Y. Jin, Retention and transport of amphiphilic colloids under unsaturated flow conditions: Effect of particle size and surface property, *Environ. Sci. Technol.*, 2005, **39,** 7853−7859.

S3. R. Kretzschmar, K. Barmettler, D. Grolimund, Y.D. Yan, M. Borkovec and H. Sticher, Experimental determination of colloid deposition rates and collision efficiencies in natural porous media, *Water Resour. Res.*, 1997, **33,** 1129−1137.

S4. Y.G. Wang, Y.S. Li, J.D. Fortner, J.B. Hughes, L.M. Abriola and K.D. Pennell, Transport and retention of nanoscale C_{60} aggregates in water-saturated porous media, *Environ. Sci. Technol.*, 2008, **42,** 3588−3594.

S5. M. Elimelech, Predicting collision efficiencies of colloidal particles in porous media, *Water Res.*, 1992, **26,** 1−8.

S6. R. Bai and C. Tien, Particle deposition under unfavorable surface interactions, *J. Colloid Interface Sci.*, 1999, **218,** 488−499.

S7. N. Toride, F. J. Leij and M. T. van Genuchten, The CXTFIT Code for Estimating Transport Parameters from Laboratory or Field Tracer Experiments, *U.S. Salinity Laboratory, Riverside, CA, USA.*, 1999.

S8. P. Nkedi-Kizza, J. W. Bigga, H. M. Selim, M. T. V. Genuchten, P. J. Wierenga and J. M. Davidson, On the equivalence of two conceptual models for describing ion exchange during transport through an aggregated oxisol, *Water Resour. Res.*, 1984, **20**, 1123–1130.

S9. R. Wikiniyadhanee, S. Chotpantarat and S. K. Ong, Effects of kaolinite colloids on Cd^{2+} transport through saturated sand under varying ionic strength conditions: Column experiments and modeling approaches, *J. Contam. Hydrol.*, 2015, **182**, 146–156.

S10. D. Kuntz and P. Grathwohl, Comparison of steady-state and transient flow conditions on reactive transport of contaminants in the vadose soil zone, *J. Hydrol.,* 2009, **369**, 225–233.

S11. H. Chen, B. Gao, H. Li and L. Q. Ma, 2011. Effects of pH and ionic strength on sulfamethoxazole and ciprofloxacin transport in saturated porous media, *J. Contam. Hydrol.,* 2011,**126**, 29–36.